

Supporting Information

Polymer-Ag Nanocomposites with Enhanced Antimicrobial Activity against Bacterial Infection

Lin Mei,[†] Zhentan Lu,[†] Xinge Zhang,^{*,†} Chaoxing Li,^{*,†} and Yanxia Jia[‡]

[†] Key Laboratory of Functional Polymer Materials of Ministry Education, Institute of Polymer Chemistry, Nankai University, Tianjin 300071, China

[‡] National Laboratory of Biomacromolecules and Center for Biological Electron Microscopy, Institute of Biophysics, Chinese Academy of Sciences, Beijing 100101, China

*Corresponding author

Tel.: +86 22 23501645; fax: +86 22 23505598.

E-mail: zhangxinge@nankai.edu.cn (Xinge Zhang), lcx@nankai.edu.cn (Chaoxing Li).

Contents

- S1. Materials
- S2. Synthesis of PDMAEMA
- S3. Quaternization of PDMAEMA
- S4. Characterization
- S5. Minimal Inhibitory Concentration
- S6. Zone of Inhibition Test
- S7. Fluorescence Microscopic Observation
- S8. Cytotoxicity Assay
- S9. *In Vivo* Studies
- S10. Study of the Stability
- S11. ^1H NMR
- S12. FTIR
- S13. Zeta Potentials
- S14. XRD

Figure S7. Growth inhibition of *P. aeruginosa* and *S. aureus* in the presence of AgNPs@PDMAEMA-C₄ with concentration range from 0 to 1.6 $\mu\text{g/mL}$.

Figure S8. Cell viability after incubation as a function of AgNPs@PDMAEMA-C₄ concentrations determined by MTT assay for one and two days. Each value represents the mean \pm SD ($n = 5$).

Table S1. PDMAEMA synthesized with different mass ratio of reagents and the quaternization degree of corresponding PDMAEMA-C₄.

S1. Materials

Silver nitrate (AgNO_3 , Premion[®], 99.995%, metals basis, Ag 63% min) and sodium borohydride (NaBH_4 , 98% min) were purchased from Alfa Aesar (Ward Hill, MA, US). DMAEMA (98%) and 2,2'-azobis(isobutyronitrile) (AIBN, 99%) were purchased from Sigma-Aldrich (Saint Louis, MO, US). DMAEMA was filtered through an activated basic alumina column before use. AIBN was purified by recrystallization from ethanol and dried at room temperature in a vacuum oven. 4-cyanopentanoic acid dithiobenzoate (CPADB) was synthesized following a procedure available in the literature.¹ *E. coli* ATCC 8739, *P. aeruginosa* ATCC 9027, and *S. aureus* ATCC 6538 strains were provided by Department of Microbiology of Nankai University (Tianjin, China).

S2. Synthesis of PDMAEMA

PDMAEMA was synthesized by RAFT polymerization using CPADB as the chain transfer agent and AIBN as the initiator. Typically, 1.0 mL of 1,4-dioxane containing 8.4 mg of CPADB, 1.23 mg of AIBN, and 510 μ L of DMAEMA were added into a Schlenk tube. The tube was sealed, deoxygenated with nitrogen in an ice-water bath for 30 min and transferred to a 70 °C water bath. The reaction was stopped after 24 h by cooling the tube in an ice-water bath. The obtained polymer was dissolved in tetrahydrofuran, precipitated into cold hexane and dried under vacuum.

S3. Quaternization of PDMAEMA

PDMAEMA was dissolved in 10 mL of ethanol containing an excess 10-fold molar ratio amount of alkyl bromides. The reaction mixture was stirred at 70 °C under reflux for 48 h. Then PDMAEMA quaternized by alkyl bromides was dialyzed (3500 Da cutoff) for 48 h against ethanol, precipitated into cold hexane and dried under vacuum. The obtained PDMAEMA-C_n was dissolved in appropriate methanol for further use. The quaternization degree was estimated by elemental analysis.

S4. Characterization

Proton nuclear magnetic resonance (^1H NMR) spectra were recorded using a Bruker AVANCE III 400MHz NMR spectrometer. The solvent was methanol- d_4 . FT-IR spectra were measured on a Fourier Transform Infrared Spectrometer (Bio-Rad, FTS6000) using a KBr tablet containing sample powder. The UV-vis absorption spectra were recorded on a UV-vis spectrophotometer (Shimadzu, UV-2550) using quartz cell with the path length of 1.0 cm. Transmission electron microscope (TEM) images were obtained using a transmission electron microscope (FEI, Tecnai G2 F20 U-TWIN) operating at 200 kV. The samples for the TEM measurements were prepared by placing a drop of AgNPs@PDMAEMA- C_4 colloid on a carbon-coated copper grid. X-ray diffract was analyzed on an X-ray diffractometer (Rigaku, D/max-2500) operated at 60 kV and 300 mA. The molecular weight and the polydispersity index (PDI) of the polymers were measured by gel permeation chromatography (GPC, Waters 1525) system equipped with triple detection array. Zeta potential was determined with Zetasizer (Malvern, Nano ZS90).

S5. Minimal Inhibitory Concentration

MIC of the nanoparticles that inhibited visible growth of the bacteria in a broth dilution susceptibility test was determined according to the guideline of the Clinical and Laboratory Standards Institute with a modified method.² The bacteria were grown overnight in Luria-Bertani (LB) broth at 37°C and subsequently diluted with LB broth to approximately 2.0×10^6 CFU/mL. The fast-growing bacterial suspension was mixed with an equal volume of 2-fold diluted antimicrobial material solution and incubated overnight at 37°C. The visible growth of the bacterial cells was assessed by measuring an optical density at 600 nm (OD_{600}) using UV-vis spectroscopy. The lowest concentration was the one at which there was no turbidity greater than the faint turbidity. Each assay was carried out in triplicate.

S6. Zone of Inhibition Test

The bacteria were incubated in LB broth at 37°C overnight. The resulting bacterial suspension was diluted to approximate 1.0×10^7 CFU/mL with LB broth. Subsequently, 50 µL of the bacterial suspension were inoculated evenly on LB agar plates. Then, the sample disk containing the antimicrobial materials was gently placed at the center of the LB agar plates. After allowing the bacteria to grow overnight at 37°C, areas of clear media surrounding the disks indicate that the antimicrobial materials inhibited bacterial growth. The antibacterial activity was measured by evaluating the diameter of the zone of inhibition around the disk.

S7. Fluorescence Microscopic Observation

The fast-growing bacterial (1.5 mL, 5.0×10^7 CFU/mL) were centrifuged at 5000 rpm for 5 min and washed by phosphate buffer solution (PBS, 0.01 mol/L, pH 7.4) three times. The supernatant was removed and the remaining bacteria were resuspended in 1.5 mL of PBS. The bacteria were treated with 100 μ L of 32 μ g/mL AgNPs@PDMAEMA- C_4 for 20 min. Then 100 μ L of fluorescent dyes were added and stained in the dark for 15 min. The fluorescent dyes were obtained by mixing 10 mg of acridine orange (AO) and 10 mg of ethidium bromide (EB) in 10 mL of PBS. After staining, the bacterial cells were rinsed with PBS three times and imaged using an inverted fluorescence microscope (Zeiss, Axiovert 200). The untreated bacterial cells were used as control.

S8. Cytotoxicity Assay

Cytotoxicity of AgNPs@PDMAEMA- C_4 was evaluated using NIH3T3 cell. The cells were cultured in Dulbecco's modified Eagles medium in a humidified atmosphere (5% CO₂, and 95% O₂). The cells were seeded into 96-well plates at about 5,000 cells per well and further incubated for 24 h at 37 °C. The nanoparticle solution was diluted with culture medium to give the final concentrations from 0.5 to 8.0 µg/mL. Then the medium in the wells was replaced with the sample suspensions. After the cells were incubated for another 24 and 48 h, 10 µL of 5% MTT solution was added into each well and the cells were incubated for further 4 h. Then the culture medium containing MTT was removed and 100 µL of dimethyl sulfoxide was added into each well to dissolve the formazan crystals with low-speed shaking for 15 min. The OD₅₄₅ value was measured using a microplate reader. The untreated cells were used as positive control and their proliferation rate was set to 100%.

S9. *In Vivo* Studies

Male Wistar rats (healthy and diabetic rats) were provided from the Chinese Academy of Medical Sciences Laboratory Animal Center, and all the protocols for animal experiment were carried out according to the guidelines of Council for the Purpose of Control and Supervision of Experiments on Animals, Ministry of Public Health, Government of China.

The rats were individually housed in cages under constant temperature with ad libitum access to food and water. The animals were anesthetized using 10% chloral hydrate (30 mg/kg) via an abdominal cavity injection. Subsequently, two quadrate (1.0×1.0 cm) and full-thickness dermal wounds were made on the left and right part of the backbone of each rat using an operating knife blade, respectively. Four wounds of each rat ($n = 14$) were covered by dressings soaked with saline and divided into four groups according to different treatments administered: Group I (treatment group), Group II (model group), Group III (drug control group), and Group IV (blank control group), respectively (Figure S1). To the wounds of Groups I and II, 100 μ L of the bacterial suspension (mixture of equal volume and concentration of *P. aeruginosa* and *S. aureus*, 2.0×10^7 CFU/mL) were applied; after 3 postoperative days, secretion of yellowish pus induced by the infected tissue was observed on these wounds of the rats. For Groups I and III, 50 μ L of 32 μ g/mL AgNPs@PDMAEMA- C_4 were administered to the wounds once a day and continued for 24 days. The wounds of Group IV were treated with 50 μ L of 0.9% NaCl solution every day, whereas the wounds of Group II were untreated. In each group, pathology observations were carried out on rats that

were sacrificed 24 days after the treatment. Tissue samples were taken from the wounds to prepare pathological slides and were observed under a Nikon Eclipse TE2000-U microscope.

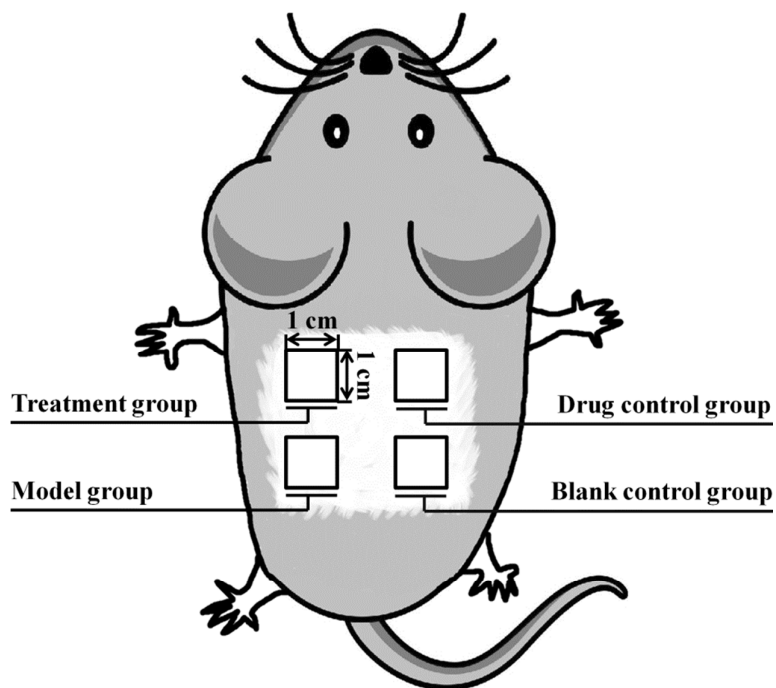


Figure S1. Diagrammatic sketch of four wounds with different treatments in a rat.

S10. Study of the Stability

From previous literatures, polymer-stabilized metal nanoparticles prepared in aqueous solution were stable for only several days.^{3,4} In the present work, AgNPs@PDMAEMA- C_n was synthesized in methanol and subsequently redispersed in aqueous solution after removed methanol, resulting in significantly increasing stabilization up to a year. In polymer-noble metal nanocomposites, the polymer can induce ordering and anisotropic orientation of the noble metal nanoparticles.⁵ The hydrophilic chain of the linear polymer PDMAEMA- C_n was expected to shrink in the methanol so that it was advantageous to the formation of nanoparticle.⁶ When the hydrophilic chain was unfolded in aqueous solution, the nanoparticle surface always remained more excellent spatial configuration comparing with its direct synthesis in aqueous solution. The hydrophilic shell of the AgNPs@PDMAEMA- C_n from the shrink to unfolding state is supported by dynamic light scattering measurement in methanol and water, respectively. Analysis of the nanoparticles in methanol gave a peak diameter of 58.8 nm, whereas that in water was 220.2 nm (Figure S2).

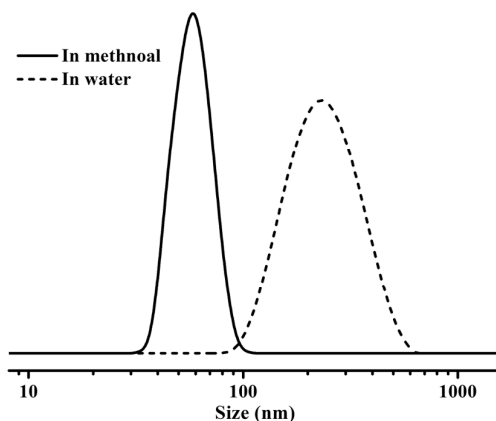


Figure S2. Size distributions of AgNPs@PDMAEMA- C_4 in methanol and water determined by DLS at 25 °C.

S11. ^1H NMR

Figure S3 exhibits the ^1H NMR spectra of PDMAEMA before quaternization (A) and after quaternization with 1-butyl bromide (B). The signals at 3.1 and 3.35 ppm were appeared after quaternization, corresponding to the methyl groups ($\text{CH}_3\text{-N}^+\text{-CH}_3$) and the methylene protons ($\text{-CH}_2\text{-N}^+\text{-CH}_2\text{-}$). The chemical shift of the methylene protons ($\text{-CO-O-CH}_2\text{-}$) increased from 4.1 to 4.5 ppm. Moreover, the peaks at 1.47 and 1.05 ppm referred to the characteristic of the ($\text{-CH}_2\text{-}$) of the long alkyl chains and the terminal methyl of the alkyl chain, respectively, indicating the presence of the long alkyl chains on the pendant amino groups of the PDMAEMA.

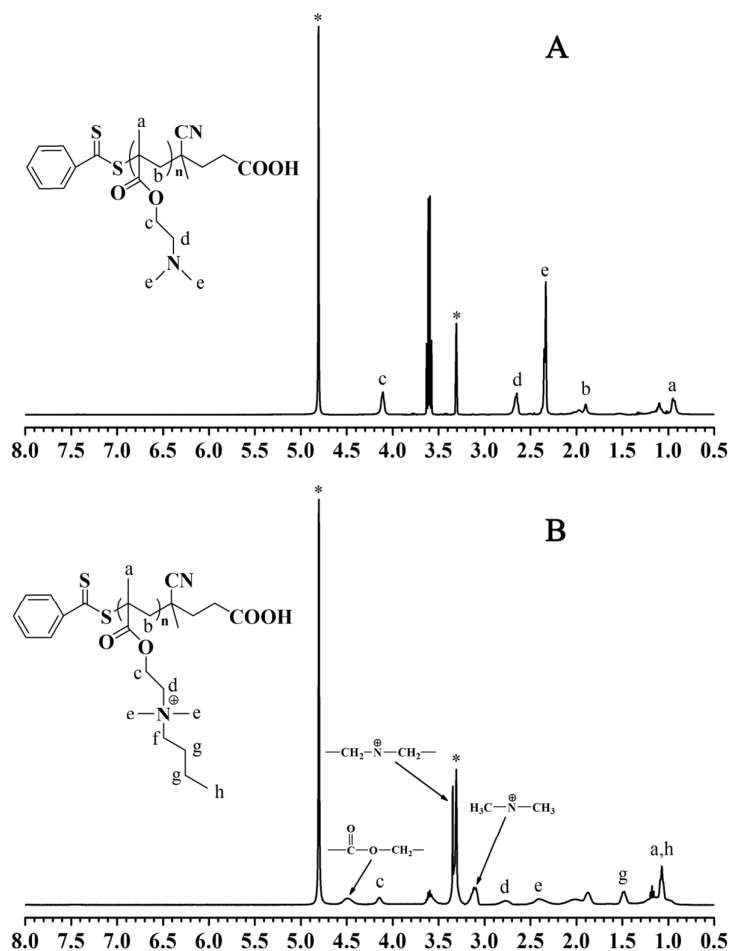


Figure S3. ^1H NMR spectra of PDMAEMA (A) and PDMAEMA- C_4 (B).

S12. FTIR

To further confirm the quaternization of PDMAEMA, FTIR assay was carried out. As shown in Figure S4, the increase of peak intensity of C-H stretching (2924 cm^{-1}) and C-N stretching (1151 cm^{-1}) in the IR spectrum of PDMAEMA- C_4 suggested the successful introduction of alkyl chain to PDMAEMA. When compared with the spectrum of PDMAEMA- C_4 , the peak of AgNPs@PDMAEMA- C_4 at 616 cm^{-1} assigned to C-S stretching was vanished, indicating that the binding of PDMAEMA- C_4 to AgNPs was mainly generated via thiol group from the reduction of PDMAEMA- C_4 .³

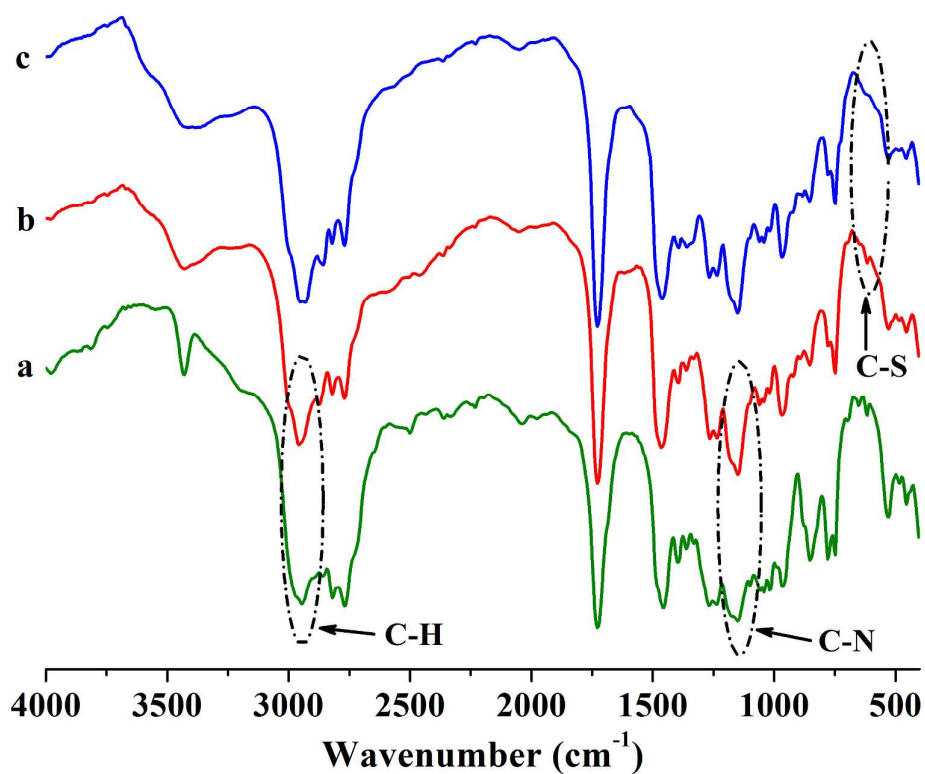


Figure S4. FTIR spectra of PDMAEMA (a), PDMAEMA- C_4 (b) and AgNPs@PDMAEMA- C_4 (c).

S13. Zeta potentials

The zeta potentials of AgNPs, AgNPs@PDMAEMA and AgNPs@PDMAEMA-C₄ were measured, and the results were shown in Figure S5. The AgNPs was inherently negative charge. When PDMAEMA was bound to the surface of AgNPs, the zeta potential of AgNPs@PDMAEMA changed from negative charge to positive charge. However, the charge of the nanoparticles dramatically increased after the fixation of PDMAEMA-C₄ on AgNPs surface, up to 32.2 mV. The higher positive charge of the nanoparticle significantly attached to the surface-negative charge on bacteria.

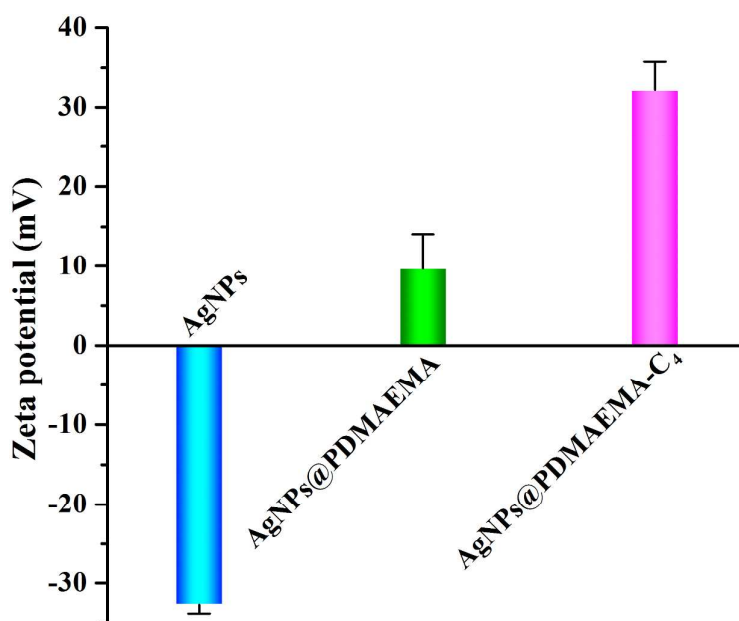


Figure S5. Zeta potential values of AgNPs, AgNPs@PDMAEMA and AgNPs@PDMAEMA-C₄.

S14. XRD

The crystalline structure of the obtained AgNPs@PDMAEMA- C_4 was further investigated from XRD analysis. Figure S6 showed the XRD pattern of the dried AgNPs@PDMAEMA- C_4 powder. Four peaks were observed at 38.12° , 43.66° , 64.39° , and 77.25° , and can be assigned to (111), (200), (220), and (311) reflections, respectively. The XRD pattern confirms that the synthesized AgNPs@PDMAEMA- C_4 was in the face-centered cubic structure (metallic Ag, JCPDS file: 65-2871).

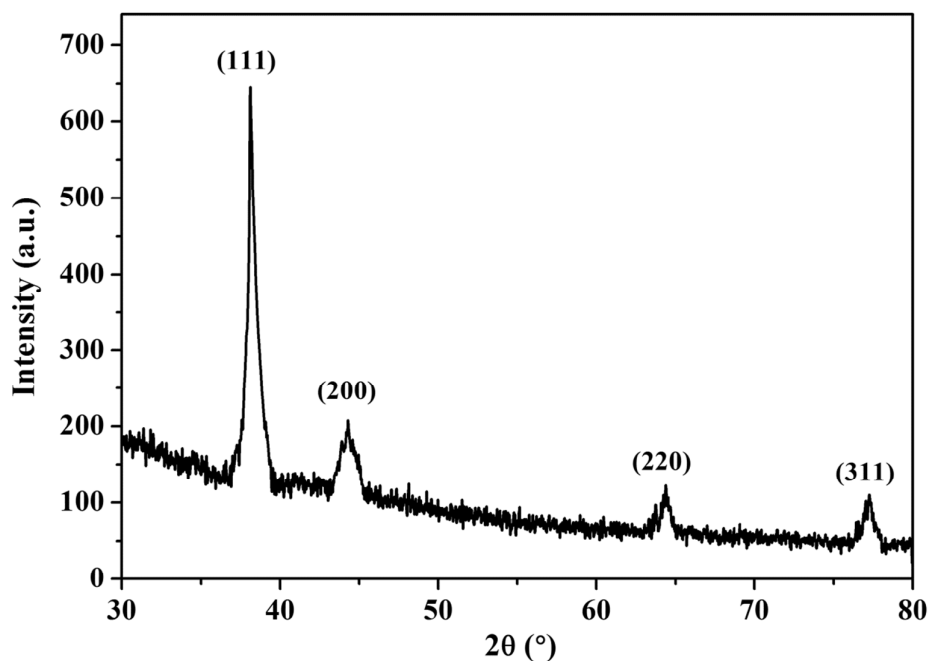


Figure S6. XRD pattern of AgNPs@PDMAEMA- C_4 powder.

Figure S7. Growth inhibition of *P. aeruginosa* and *S. aureus* in the presence of AgNPs@PDMAEMA- C_4 with concentration range from 0 to 1.6 $\mu\text{g/mL}$.

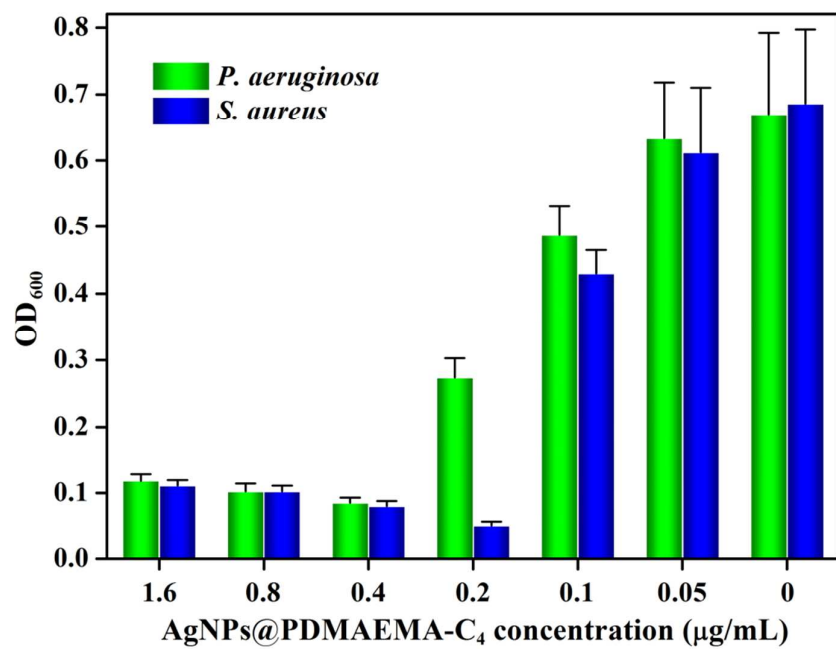


Figure S8. Cell viability after incubation as a function of AgNPs@PDMAEMA-C₄ concentrations determined by MTT assay for one and two days. Each value represents the mean \pm SD ($n = 5$).

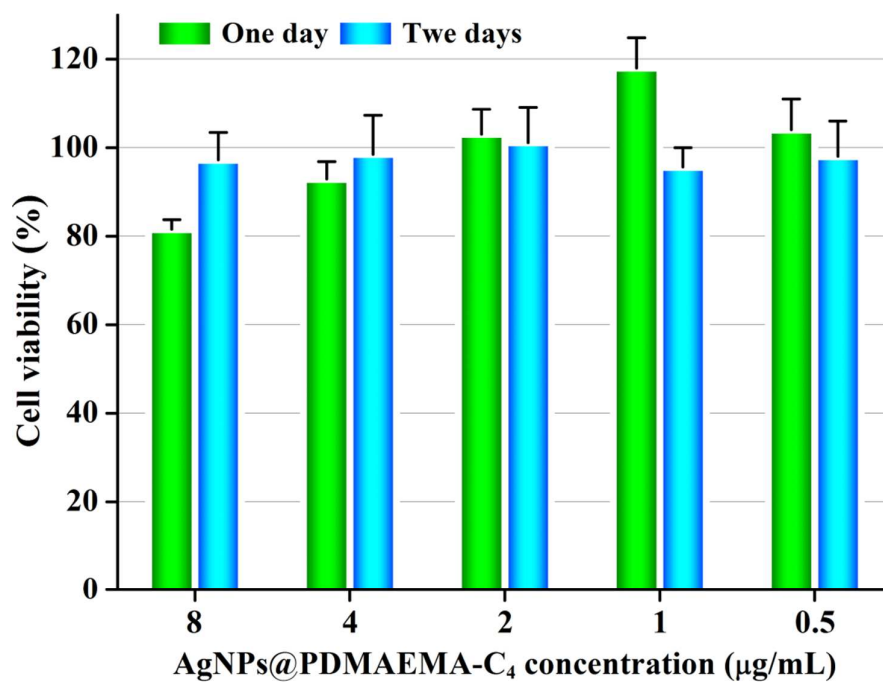


Table S1. PDMAEMA synthesized with different mass ratio of reagents and the quaternization degree of corresponding PDMAEMA-C₄.

DMAEMA (mL)	CPADB (mg)	AIBN (mg)	Mn (Daltons)	PDI	Quaternization degree (%)
1.0	16.8	2.5	8247	1.25	81.3
2.0	16.8	2.5	17430	1.18	80.1
2.0	8.4	1.3	24310	1.15	76.3
3.5	8.4	1.3	31724	1.15	72.2

References and Notes

- (1) Mitsukami, Y.; Donovan, M. S.; Lowe, A. B.; McCormick, C. L. Water-soluble Polymers. 81. Direct Synthesis of Hydrophilic Styrenic-based Homopolymers and Block Copolymers in Aqueous Solution via RAFT. *Macromolecules* **2001**, *34*, 2248–2256.
- (2) Clinical and Laboratory Standards Institute. Methods for Dilution Antimicrobial Susceptibility Tests for Bacteria That Grow Aerobically; Approved Standard—Seventh Edition. Clinical and Laboratory Standards Institute document M7-A7 [ISBN 1-56238-587-9]. Clinical and Laboratory Standards Institute, 940 West Valley Road, Suite 1400, Wayne, Pennsylvania 19087-1898 USA, 2006.
- (3) Lowe, A. B.; Sumerlin, B. S.; Donovan, M. S.; McCormick, C. L. Facile Preparation of Transition Metal Nanoparticles Stabilized by Well-defined (Co)Polymers Synthesized via Aqueous Reversible Addition-fragmentation Chain Transfer Polymerization. *J. Am. Chem. Soc.* **2002**, *124*, 11562–11563.
- (4) Sambhy, V.; MacBride, M. M.; Peterson, B. R.; Sen, A. Silver Bromide Nanoparticle/Polymer Composites: Dual Action Tunable Antimicrobial Materials. *J. Am. Chem. Soc.* **2006**, *128*, 9798–9808.
- (5) Shenhar, R.; Norsten, T. B.; Rotello, V. M. Polymer-mediated Nanoparticle Assembly: Structural Control and Applications. *Adv. Mater.* **2005**, *17*, 657–669.
- (6) Wang, K.; Peng, H.; Thurecht, K. J.; Puttick, S.; Whittaker, A. K. pH-responsive Star Polymer Nanoparticles: Potential ^{19}F MRI Contrast Agents for

Tumour-selective Imaging. *Polym. Chem.* **2013**, 4, 4480–4489.